View metadata, citation and similar papers at core.ac.uk

brought to you by CORE

provided by Online Research Database In Technology

Technical University of Denmark

Ultrasound fields from triangular apertures

Jensen, Jørgen Arendt

Published in:
Acoustical Society of America. Journal

Link to article, DOI:
10.1121/1.417914

Publication date:
1996

Document Version
Publisher's PDF, also known as Version of record

Link back to DTU Orbit

Citation (APA):
Jensen, J. A. (1996). Ultrasound fields from triangular apertures. Acoustical Society of America. Journal, 100(4), 2049-2056. DOI: 10.1121/1.417914

DTU Library
Technical Information Center of Denmark

General rights
Copyright and moral rights for the publications made accessible in the public portal are retained by the authors and/or other copyright owners and it is a condition of accessing publications that users recognise and abide by the legal requirements associated with these rights.

- Users may download and print one copy of any publication from the public portal for the purpose of private study or research.
- You may not further distribute the material or use it for any profit-making activity or commercial gain
- You may freely distribute the URL identifying the publication in the public portal

If you believe that this document breaches copyright please contact us providing details, and we will remove access to the work immediately and investigate your claim.

Ultrasound fields from triangular apertures

Jørgen Arendt Jensen
Department of Information Technology, Building 344, Technical University of Denmark, DK-2800 Lyngby, Denmark

(Received 18 October 1995; revised 15 March 1996; accepted 25 March 1996)

The pulsed field from a triangular aperture mounted in an infinite, rigid baffle is calculated. The approach of spatial impulse responses, as developed by Tupholme and Stepanishen, is used. By this both the emitted and received pulsed ultrasound field can be found for any transducer excitation and electromechanical impulse response. The continuous wave field is also readily obtainable through a simple Fourier transform. The spatial impulse response is calculated without approximation, and the solution is valid in the half-space in front of the aperture for a homogeneous, nonattenuating medium. The solution can be used in finite element programs for calculating fields from arbitrary transducer geometries. © *1996 Acoustical Society of America.*

PACS numbers: 43.20.Rz, 43.20.Px, 43.35.Wa [JEG]

INTRODUCTION

The medical ultrasound scanners of today increasingly use advanced transducer geometries for creating ultrasound fields suitable for probing the human body. Different types of one-dimensional and 1.5- and 2-D arrays are used. Apodizing of elements and weighting between elements are used for decreasing sidelobes and increasing the depth of field. A first characterization of these transducers and their optimization is based on computer simulation of the fields. One possible method for making a simulation is to split the transducer aperture into squares and sum the individual responses to yield the field.[1] This works well for array transducers with square elements, but an inordinate amount of elements must be used for circular transducers and annular arrays. A better choice of elementary subdivision would be to use a triangularly shaped element, since this better fits circular shapes. Thereby a smaller number of elements are used, which can lead to shorter computation times. Unfortunately the field has not been calculated for this type of element, and that has hampered the development of such a simulation program. This paper presents a full calculation of the field from a triangular aperture.

A number of different methods for calculating ultrasound fields exists.[2] The most powerful approach seems to be the one developed by Tupholme and Stepanishen.[3–5] They derived a method for determining the spatial impulse response of an aperture, yielding the time response received at a specific point in space for a given transducer surface velocity. The approach relies on linear systems theory and assumes the ultrasound propagation to be linear and to take place in a nonattenuating, homogeneous medium. The field is found with no approximations, if the aperture is flat and is mounted in an infinite rigid baffle. For slightly curved transducers the solution is still applicable, if the radius of curvature is large compared to the wavelength of the ultrasound field. It is, thus possible with this method to calculate the spatially nonstationary field for all points and for all time, and for any transducer surface velocity.

A number of authors have derived equations for the spatial impulse response for different apertures. Stepanishen[4] derived the response for a flat, circular aperture, and Penttinen and Luukkala[6] and Arditi *et al.*[7] gave equations for radiation from a concave transducer. The field from a rectangular aperture has been derived by Lockwood and Willette.[8]

I. BASIC THEORY

The basic setup is shown in Fig. 1. The triangularly shaped aperture is placed in an infinite, rigid baffle on which the velocity normal to the plane is zero, except at the aperture. The field point is denoted by $\mathbf{r}_1$ and the aperture by $\mathbf{r}_2$. The pressure field generated by the aperture is then found by the Rayleigh integral[9]

$$p(\mathbf{r}_1,t)=\frac{\rho_0}{2\pi}\int_S \frac{\partial v_n(\mathbf{r}_2,t-|\mathbf{r}_1-\mathbf{r}_2|/c)/\partial t}{|\mathbf{r}_1-\mathbf{r}_2|}\,dS, \tag{1}$$

where v_n is the velocity normal to the transducer surface, c is the speed of sound, and ρ is the density of the medium. The integral is a statement of Huyghen's principle that the field is found by integrating the contributions from all the infinitesimally small area elements that make up the aperture. This integral formulation assumes linearity and propagation in a homogeneous medium without attenuation. Further, the radiating aperture is assumed flat, so no reradiation takes place. Exchanging the integration and the partial derivative, the integral can be written as

$$p(\mathbf{r}_1,t)=\frac{\rho_0}{2\pi}\,\partial\int_S \frac{v_n(\mathbf{r}_2,t-|\mathbf{r}_1-\mathbf{r}_2|/c)}{|\mathbf{r}_1-\mathbf{r}_2|}\,\frac{dS}{\partial t}. \tag{2}$$

It is convenient to introduce the velocity potential ψ that satisfies the equations[10]

$$\mathbf{v}(\mathbf{r},t)=-\nabla\psi(\mathbf{r},t),\quad p(\mathbf{r},t)=\rho_0\,\frac{\partial\psi(\mathbf{r},t)}{\partial t}. \tag{3}$$

The convenience of introducing this potential function is that only a scalar quantity need be calculated, and that all field quantities can be derived from it. The surface integral is then equal to the velocity potential:

$$\psi(\mathbf{r}_1,t)=\int_S \frac{v_n(\mathbf{r}_2,t-|\mathbf{r}_1-\mathbf{r}_2|/c)}{2\pi|\mathbf{r}_1-\mathbf{r}_2|}\,dS. \tag{4}$$

Downloaded¬28¬Jun¬2010¬to¬192.38.67.112.¬Redistribution¬subject¬to¬ASA¬license¬or¬copyright;¬see¬http://asadl.org/journals/doc/ASALIB-home/info/ter

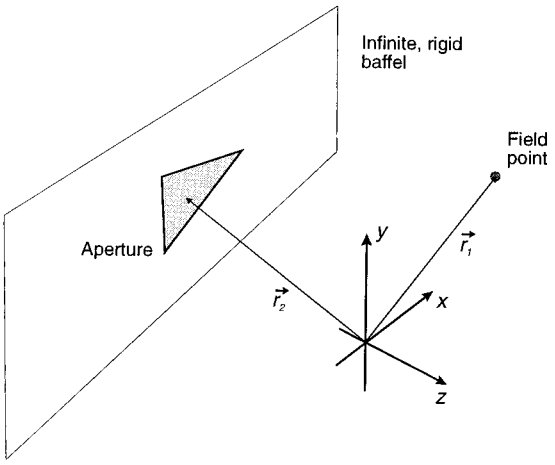

FIG. 1. Position of transducer, field point, and coordinate system.

The excitation pulse can be separated from the transducer geometry by introducing a time convolution with a delta function as

$$\psi(\mathbf{r}_1,t)=\int_S\int_T \frac{v_n(\mathbf{r}_2,t_2)\,\delta(t-t_2-|\mathbf{r}_1-\mathbf{r}_2|/c)}{2\pi|\mathbf{r}_1-\mathbf{r}_2|}\,dt_2\,dS, \tag{5}$$

where δ is the Dirac delta function. Assume now that the surface velocity is uniform over the aperture making it independent of $\mathbf{r}_2$, then

$$\psi(\mathbf{r}_1,t)=v_n(t)*\int_S \frac{\delta(t-|\mathbf{r}_1-\mathbf{r}_2|/c)}{2\pi|\mathbf{r}_1-\mathbf{r}_2|}\,dS, \tag{6}$$

where $*$ denotes convolution in time. The integral in this equation

$$h(\mathbf{r}_1,t)=\int_S \frac{\delta(t-|\mathbf{r}_1-\mathbf{r}_2|/c)}{2\pi|\mathbf{r}_1-\mathbf{r}_2|}\,dS \tag{7}$$

is called the spatial impulse response and characterizes the three-dimensional extent of the field for a particular transducer geometry. Note that this is a function of the relative position between the aperture and the field. The calculation assumes linearity and any complex-shaped transducer can therefore be divided into smaller apertures and the response found by adding the responses from the subapertures. The integral can be seen as a statement of Huyghen's principle of summing contributions from all areas of the aperture. A second interpretation is found from using the acoustic reciprocity theorem,[11] which says that source and receiver can be interchanged. Emitting a spherical wave from the field point and finding the wave's intersection with the aperture also yields the spatial impulse response. This is the approach used in this paper.

Using the spatial impulse response the pressure is written as

$$p(\mathbf{r}_1,t)=\rho\,\frac{\partial v_n(t)}{\partial t}*h(\mathbf{r}_1,t), \tag{8}$$

which equals the emitted pressure. The continuous wave field can be found from the Fourier transform of (8). The

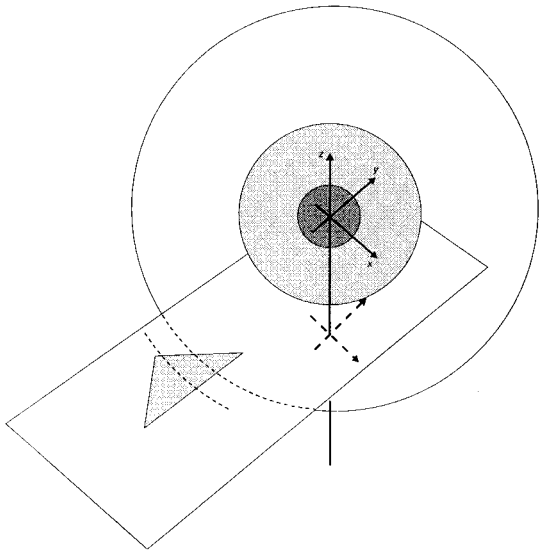

FIG. 2. Emission of spherical wave from the field point and its intersection of the triangle.

received response for a collection of scatterers can also be found from the spatial impulse response.[12,13] Thus the calculation of the spatial impulse response makes it possible to find all ultrasound fields of interest.

II. GEOMETRIC CONSIDERATIONS

The spatial impulse response is found by emitting a spherical wave from the field point and then find the intersection of the wave and the triangle. The situation is depicted in Fig. 2. The calculation of the impulse response is eased by projecting the field point onto the plane of the triangle. The task is then reduced to a two-dimensional problem and the field point is given as a (x,y) coordinate set and a height z above the plane. The three-dimensional spherical waves are then reduced to circles in the x-y plane with origo at the position of the projected field point.

The situation is shown in Fig. 3. The spatial impulse response is determined by the relative length of the part of the arc that intersects the triangle (see Sec. III), and quite a number of different intersections between the wave and the

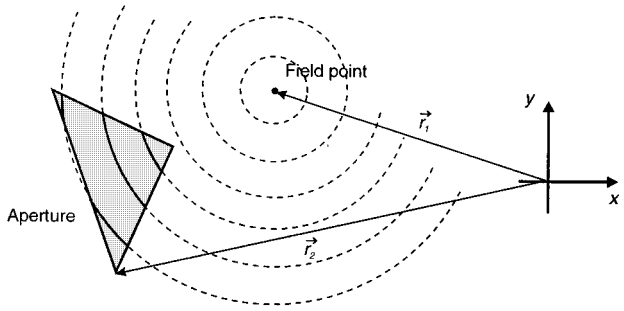

FIG. 3. Intersection of spherical waves from the field point by the triangle, when the field point is projected onto the plane of the triangle.

Downloaded¬28¬Jun¬2010¬to¬192.38.67.112.¬Redistribution¬subject¬to¬ASA¬license¬or¬copyright;¬see¬http://asadl.org/journals/doc/ASALIB-home/info/ter

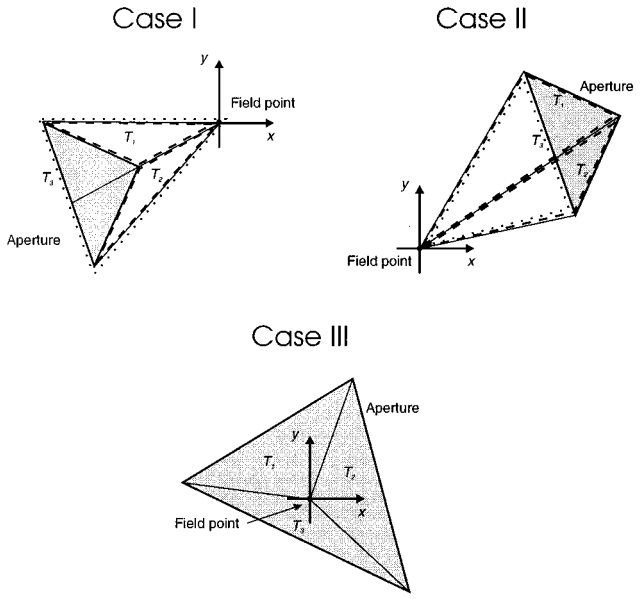

FIG. 4. Triangles used for calculating the spatial impulse response.

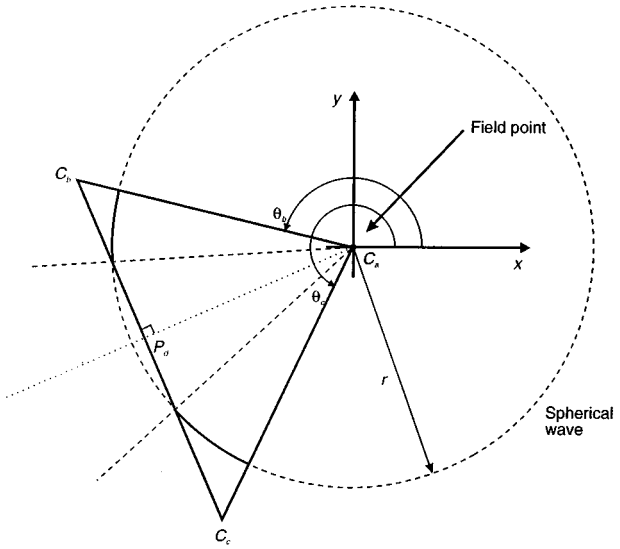

FIG. 5. Position of triangle and field point.

triangle can arise making the evaluation cumbersome. The calculation is therefore eased by introducing three new triangles as shown in Fig. 4. All three triangles have one corner point at the field point, and the other points are given by the corner points of the aperture. The response of the aperture is then found as a linear combination of the three responses due to the linear propagation. The triangles T_1 and T_2 are indicated by dashed lines, T_3 by a dotted line, and the aperture by a solid line. The spatial impulse response of each of these triangles is derived in the next section.

Three different cases exists for the orientation of the triangles as shown in Fig. 4. The spatial impulse response of the aperture is in case I given by

$$h(\mathbf{r}_1,t)=h_{T_3}(\mathbf{r}_1,t)-h_{T_1}(\mathbf{r}_1,t)-h_{T_2}(\mathbf{r}_1,t). \tag{9}$$

Here triangle T_3 have corner points at the edges of the aperture, and T_1 and T_2 are formed by a dividing line through the center point of the aperture and the lines to the two edges (see Fig. 4). The response in case II is

$$h(\mathbf{r}_1,t)=h_{T_1}(\mathbf{r}_1,t)+h_{T_2}(\mathbf{r}_1,t)-h_{T_3}(\mathbf{r}_1,t). \tag{10}$$

The response is

$$h(\mathbf{r}_1,t)=h_{T_1}(\mathbf{r}_1,t)+h_{T_2}(\mathbf{r}_1,t)+h_{T_3}(\mathbf{r}_1,t) \tag{11}$$

in case III, where the field point is inside the triangle.

The problem is hereby reduced to finding the response from a triangle, where the field point is positioned at one of the edges.

III. SPATIAL IMPULSE RESPONSE AT A CORNER POINT

The position of the triangle and the field point along with associated variables are shown in Fig. 5. The origo of the coordinate system is placed at the field point and coincides with one of the triangles corner points. The spherical waves are also centered at origo. The corner points are denoted by C_a, C_b, and C_c, i.e., $C_a=(x_a,y_a)$.

The spatial impulse response is given by the surface integral

$$h(\mathbf{r}_1,t)=\int_S \frac{\delta(t-|\mathbf{r}_1-\mathbf{r}_2|/c)}{2\pi|\mathbf{r}_1-\mathbf{r}_2|}\,dS, \tag{12}$$

where $\mathbf{r}_1$ indicates the position of the field point and $\mathbf{r}_2$ the position on the aperture. Conversion to a polar coordinate system is given by

$$\int\int_S f(x,y)dx\,dy=\int_0^r\int_0^{2\pi} rf(r,\theta)d\theta\,dr. \tag{13}$$

The projected circles have a radius of r and the distance to the field point is thus

$$R=\sqrt{z^2+r^2}, \tag{14}$$

where z is the field point's height above the x-y plane. The relation between time and radius is

$$r=\sqrt{(ct)^2-z^2}. \tag{15}$$

The integral is then

$$h(\mathbf{r}_1,t)=\int_0^r\int_0^{2\pi} r\,\frac{\delta(t-|R|/c)}{2\pi|R|}\,d\theta\,dr. \tag{16}$$

The spatial impulse response is dependent on the arrival time of the spherical waves at the triangle. The response is zero until the first response arrives at time $t=t_1=z/c$, hereafter the fixed part of the circle between the angles θ_b and θ_c contributes to the response. The impulse response changes when either the point P_d or the corner point C_b or C_c is reached, whichever is closest. Until these points the spatial impulse response is given by

Downloaded¬28¬Jun¬2010¬to¬192.38.67.112.¬Redistribution¬subject¬to¬ASA¬license¬or¬copyright;¬see¬http://asadl.org/journals/doc/ASALIB-home/info/ter

$$h_T(\mathbf{r}_1,t)=\int_0^r\int_{\theta_b}^{\theta_c} r\,\frac{\delta\left(t-\frac{|R|}{c}\right)}{2\pi|R|}\,d\theta\,dr$$

$$=\frac{\theta_c-\theta_b}{2\pi}\int_0^r r\,\frac{\delta\left(t-\frac{|R|}{c}\right)}{|R|}\,dr \tag{17}$$

with the angles defined in Fig. 5. Introducing the substitution $2R\,dR=2r\,dr$ gives [see Eq. (14)]

$$h_T(\mathbf{r}_1,t)=\frac{\theta_c-\theta_b}{2\pi}\int_z^{\sqrt{z^2+r^2}} R\,\frac{\delta(t-|R|/c)}{|R|}\,dR$$

$$=\frac{\theta_c-\theta_b}{2\pi}\int_z^{\sqrt{z^2+r^2}}\delta\left(t-\frac{|R|}{c}\right)dR \tag{18}$$

since the distance always is positive. Using the time substitution $R/c=t'$ finally results in

$$h_T(\mathbf{r}_1,t)=\frac{\theta_c-\theta_b}{2\pi}\,c\int_{z/c}^{\sqrt{z^2+r^2/c}}\delta(t-t')dt'$$

$$=\frac{\theta_c-\theta_b}{2\pi}\,c\int_{t_1}^{t_x}\delta(t-t')dt'$$

$$=\frac{(\theta_c-\theta_b)c}{2\pi}\quad\text{for } t_1\leqslant t\leqslant t_x. \tag{19}$$

The time t_x equals the corresponding time for the point closest to origo. The spatial impulse response is, thus constant until either the point C_b, C_c, or P_d is reached, and it then drops of as a function of the angle difference.

The spatial impulse response is dependent on the length of the arc intersecting the triangle, and the calculation is, thus eased by rotating the triangle so that one side runs along the x axis, and so that the other corner point always has a positive y value. The angles are given by

$$\theta_b=\arctan(y_b,x_b),\quad \theta_c=\arctan(y_c,x_c). \tag{20}$$

A four quadrant arcus tangent should be used here yielding values from 0 to 2π. If $\theta_b>\theta_c$ and $(\theta_b-\theta_c)<\pi$ then the rotation angle should be $\theta_r=\theta_c$, else if $(\theta_b-\theta_c)>\pi$ then $\theta_r=\theta_b$. The reverse is true if $\theta_b<\theta_c$ [i.e., $\theta_r=\theta_b$ for $(\theta_c-\theta_b)<\pi$]. The rotated points are then found from

$$x_n=x\,\cos(\theta_r)+y\,\sin(\theta_r),$$

$$y_n=-x\,\sin(\theta_r)+y\,\cos(\theta_r), \tag{21}$$

where (x_n,y_n) are the new coordinates in the rotated coordinate system. The different situations and the associated variables are then depicted in Fig. 6. The rotated points are called $C_1=(x_1,y_1)$, $C_2=(x_2,y_2)$, $C_3=(x_3,y_3)$, and $P_4=(x_4,y_4)$, respectively. The spatial impulse responses are easily derived when keeping in mind that it is the angle of the arc intersected by the triangle that determines the response. The arc is determined by the time through Eq. (15) and discontinuities are found in the response when one of the corner points are meet. The different arrival times are

$$t_1=\frac{z}{c},\quad t_2=\frac{\sqrt{z^2+x_2^2+y_2^2}}{c},$$

$$t_3=\frac{\sqrt{z^2+x_3^2+y_3^2}}{c},\quad t_4=\frac{\sqrt{z^2+x_4^2+y_4^2}}{c}. \tag{22}$$

The point P_4 is found as the intersection between the C_2-C_3 line and a line perpendicular to the C_2-C_3 line and going through C_1. The line C_2-C_3 is given by

$$y=\beta(x-x_2),\quad \beta=\frac{y_3}{x_3-x_2}. \tag{23}$$

The line perpendicular to this has a slope of $\alpha=-1/\beta$ and the intersection of the lines is given by

$$x_4=\frac{\beta^2 x_2}{1+\beta^2},\quad y_4=\beta(x_4-x_2). \tag{24}$$

The spatial impulse response is determined by the angles shown in Fig. 6. For situation 0 the response is

$$h_T(\mathbf{r}_1,t)=\begin{cases}0, & t_1>t,\\ \dfrac{\theta_0 c}{2\pi}, & t_1\leqslant t\leqslant t_2,\\ \dfrac{(\theta_0-\theta_3(t))c}{2\pi}, & t_2\leqslant t\leqslant t_3,\\ 0, & t_3<t,\end{cases} \tag{25}$$

where $\theta_3(t)$ is determined by the intersection of the spherical wave and the C_2-C_3 line. The angles are

$$\theta_0=\arccos\left(\frac{x_3}{\sqrt{y_3^2+x_3^2}}\right),\quad \theta_3(t)=\arccos\left(\frac{x_3}{r(t)}\right),$$

$$r(t)=\sqrt{(ct)^2-z^2}. \tag{26}$$

All other responses are determined from the angle differences shown in Fig. 6. The angles $\theta_1(t)$ and $\theta_2(t)$ are determined by the intersection of the C_2-C_3 line with the spherical wave. The angles are

$$\theta_1(t)=\arccos\left(\frac{x_2\beta^2+\sqrt{(1+\beta^2)r^2(t)-x_2^2\beta^2}}{(1+\beta^2)r(t)}\right),$$

$$\theta_2(t)=\arccos\left(\frac{x_2\beta^2-\sqrt{(1+\beta^2)r^2(t)-x_2^2\beta^2}}{(1+\beta^2)r(t)}\right). \tag{27}$$

The response for the different times and situations are then readily found. The response for situation 4 is, e.g.,

Downloaded¬28¬Jun¬2010¬to¬192.38.67.112.¬Redistribution¬subject¬to¬ASA¬license¬or¬copyright;¬see¬http://asadl.org/journals/doc/ASALIB-home/info/ter

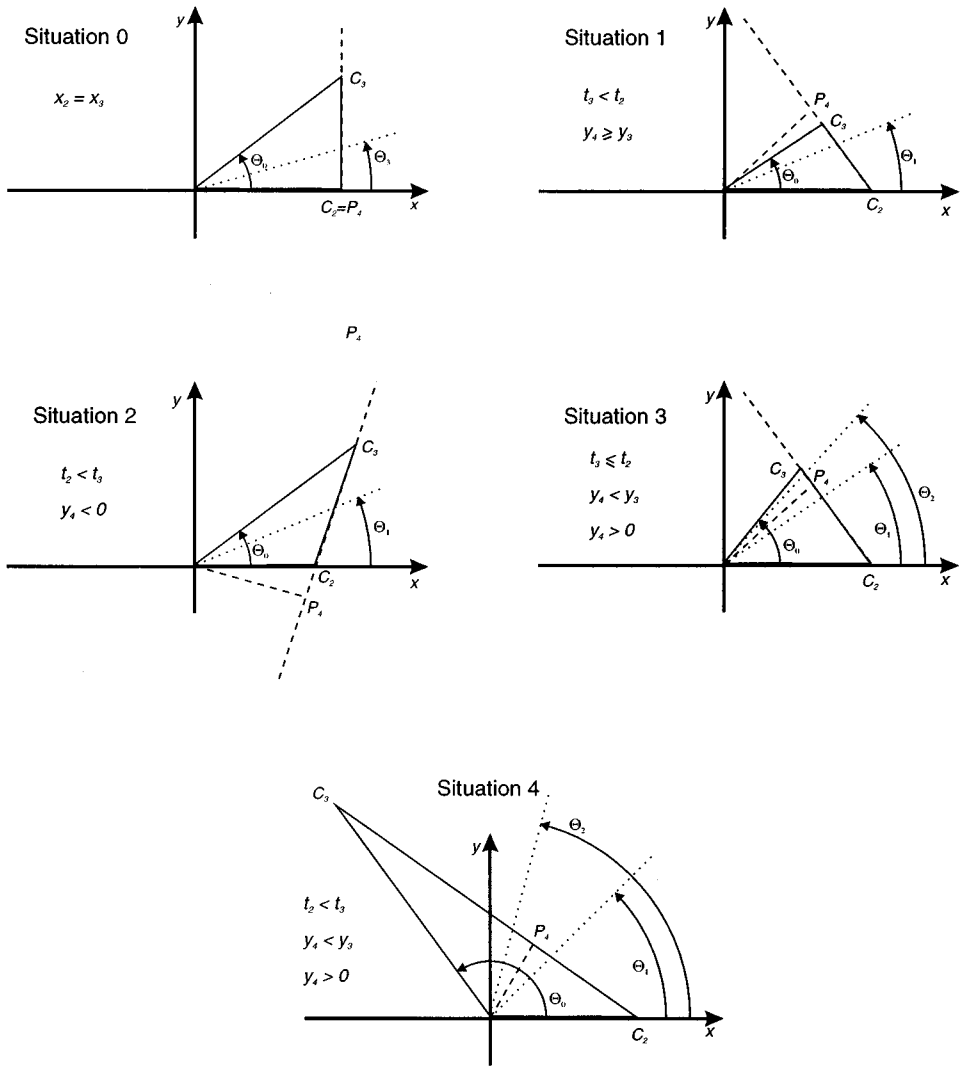

FIG. 6. The possible placements of the triangles and the field point.

$$h_T(\mathbf{r}_1,t)=\begin{cases}0, & t_1>t,\\ \dfrac{\theta_0 c}{2\pi}, & t_1\leqslant t\leqslant t_4,\\ \dfrac{[\theta_0-(\theta_2(t)-\theta_1(t))]c}{2\pi}, & t_4\leqslant t\leqslant t_2,\\ \dfrac{(\theta_0-\theta_2(t))c}{2\pi}, & t_2\leqslant t\leqslant t_3,\\ 0, & t_3<t.\end{cases} \tag{28}$$

The other situations are derived along the same lines and the complete solution is given in Sec. IV.

IV. SPATIAL IMPULSE RESPONSE OF TRIANGLE

The field point denoted by $\mathbf{r}_1$ is relative to the coordinate system, where the x and y axis lie in the plane of the triangle and the z axis is height above the plane. The definition of the different regions is shown in Fig. 7, and the various variables are defined in Fig. 4 and Fig. 6.

The complete equation for the spatial impulse response of a triangle is then given by

$$\text{case I:}\quad h(\mathbf{r}_1,t)=h_{T_3}(\mathbf{r}_1,t)-h_{T_1}(\mathbf{r}_1,t)-h_{T_2}(\mathbf{r}_1,t),$$

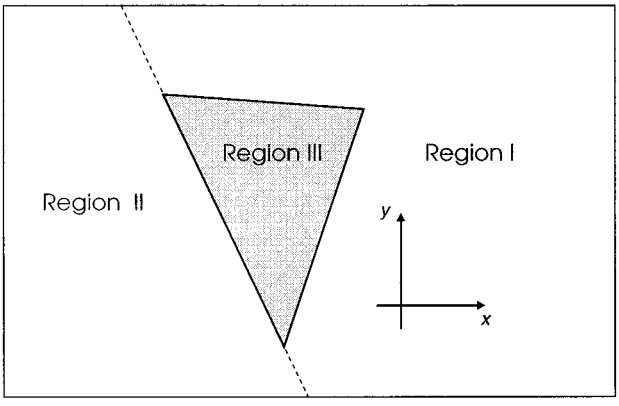

FIG. 7. Regions used in Eq. (29).

Downloaded¬28¬Jun¬2010¬to¬192.38.67.112.¬Redistribution¬subject¬to¬ASA¬license¬or¬copyright;¬see¬http://asadl.org/journals/doc/ASALIB-home/info/ter

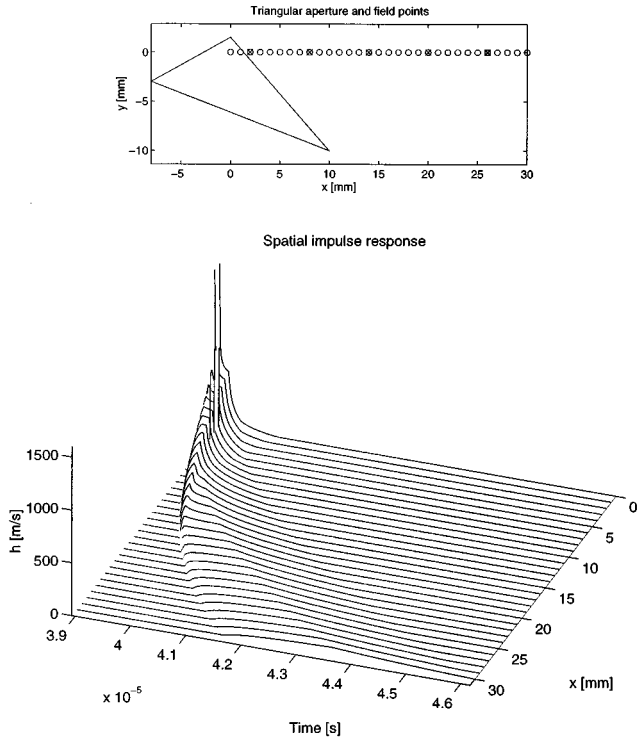

FIG. 8. Spatial impulse response of triangle. The top graph indicates the triangle position and size, and the circles indicates the field point positions for the spatial impulse responses shown in the bottom graph.

$$\text{case II:} \quad h(\mathbf{r}_1,t)=h_{T_1}(\mathbf{r}_1,t)+h_{T_2}(\mathbf{r}_1,t)-h_{T_3}(\mathbf{r}_1,t), \tag{29}$$

$$\text{case III:} \quad h(\mathbf{r}_1,t)=h_{T_1}(\mathbf{r}_1,t)+h_{T_2}(\mathbf{r}_1,t)+h_{T_3}(\mathbf{r}_1,t),$$

where $h_T(\mathbf{r},t)$ for the different situations are given by

Situation 0: $x_2=x_3$

$$h_T(\mathbf{r}_1,t)=\begin{cases}0, & t_1>t,\\ \dfrac{c}{2\pi}\,\theta_0, & t_1\leqslant t\leqslant t_2,\\ \dfrac{c}{2\pi}\,(\theta_0-\theta_3(t)), & t_2\leqslant t\leqslant t_3,\\ 0, & t_3<t.\end{cases} \tag{30}$$

Situation 1: $t_3<t_2, y_4\geqslant y_3$

$$h_T(\mathbf{r}_1,t)=\begin{cases}0, & t_1>t,\\ \dfrac{c}{2\pi}\,\theta_0, & t_1\leqslant t\leqslant t_3,\\ \dfrac{c}{2\pi}\,\theta_1(t), & t_3\leqslant t\leqslant t_2,\\ 0, & t_2<t.\end{cases} \tag{31}$$

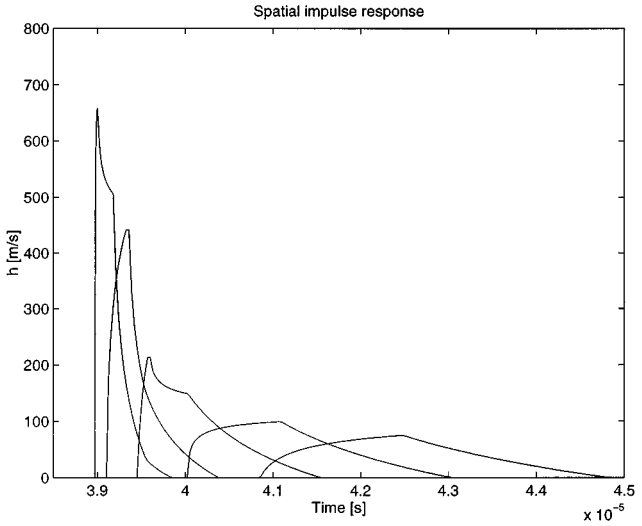

FIG. 9. Spatial impulse responses calculated for a triangle at the positions indicated by the crosses in Fig. 8.

Situation 2: $t_2<t_3, y_4<0$

$$h_T(\mathbf{r}_1,t)=\begin{cases}0, & t_1>t,\\ \dfrac{c}{2\pi}\,\theta_0, & t_1\leqslant t\leqslant t_2,\\ \dfrac{c}{2\pi}\,(\theta_0-\theta_1(t)), & t_2\leqslant t\leqslant t_3,\\ 0, & t_3<t.\end{cases} \tag{32}$$

Situation 3: $t_3\leqslant t_2, y_4<y_3, y_4>0$

$$h_T(\mathbf{r}_1,t)=\begin{cases}0, & t_1>t,\\ \dfrac{c}{2\pi}\,\theta_0, & t_1\leqslant t\leqslant t_4,\\ \dfrac{c}{2\pi}\,[\theta_0-(\theta_2(t)-\theta_1(t))], & t_4\leqslant t\leqslant t_3,\\ \dfrac{c}{2\pi}\,(\theta_0-\theta_1(t)), & t_3\leqslant t\leqslant t_2,\\ 0, & t_2<t.\end{cases} \tag{33}$$

Situation 4: $t_2<t_3, y_4<y_3, y_4>0$

$$h_T(\mathbf{r}_1,t)=\begin{cases}0, & t_1>t,\\ \dfrac{c}{2\pi}\,\theta_0, & t_1\leqslant t\leqslant t_4,\\ \dfrac{c}{2\pi}\,[\theta_0-(\theta_2(t)-\theta_1(t))], & t_4\leqslant t\leqslant t_2,\\ \dfrac{c}{2\pi}\,(\theta_0-\theta_2(t)), & t_2\leqslant t\leqslant t_3,\\ 0, & t_3<t.\end{cases} \tag{34}$$

The different variables used are given by

Downloaded¬28¬Jun¬2010¬to¬192.38.67.112.¬Redistribution¬subject¬to¬ASA¬license¬or¬copyright;¬see¬http://asadl.org/journals/doc/ASALIB-home/info/ter

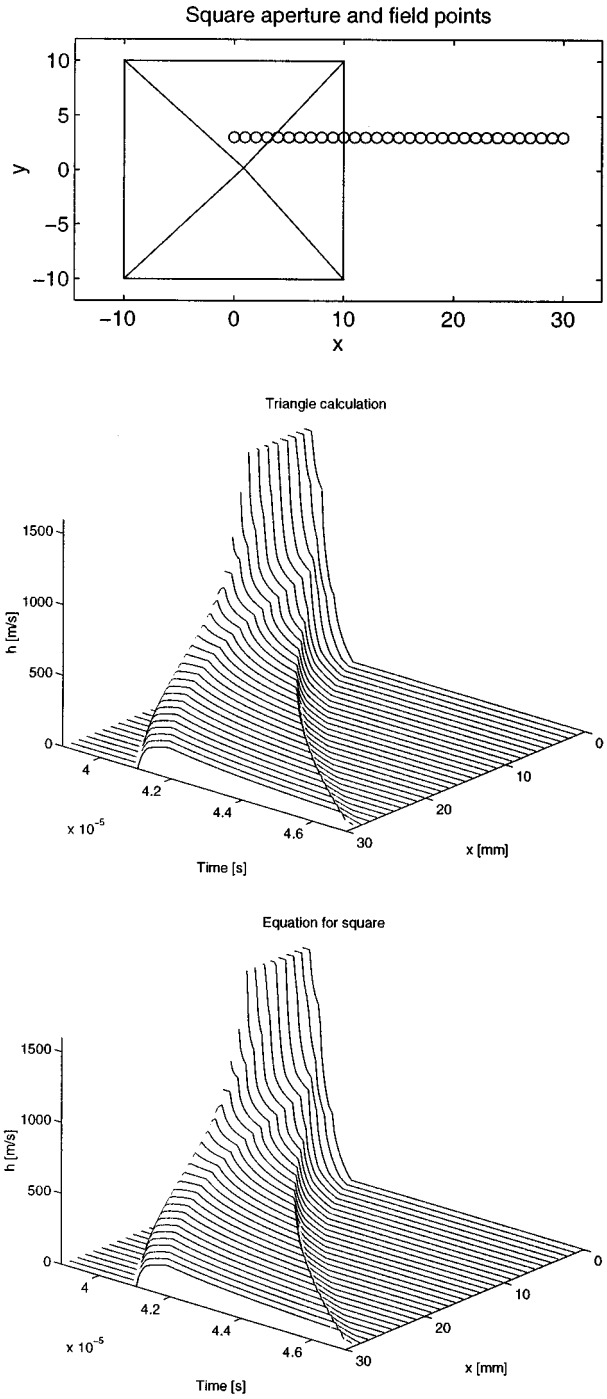

FIG. 10. Calculation of field from square element. The top graph shows the field point positions and the middle graph is the spatial impulse response calculated from the equations derived in this paper. The bottom graph is calculated from the equations for a square element.

$$t_1=\frac{z}{c},\quad t_2=\frac{\sqrt{z^2+x_2^2+y_2^2}}{c},$$

$$t_3=\frac{\sqrt{z^2+x_3^2+y_3^2}}{c},\quad t_4=\frac{\sqrt{z^2+x_4^2+y_4^2}}{c},$$

$$\beta=\frac{y_3}{x_3-x_2},\quad x_4=\frac{\beta^2 x_2}{1+\beta^2},\quad y_4=\beta(x_4-x_2),$$

$$r(t)=\sqrt{(ct)^2-z^2},\quad \theta_0=\arccos\left(\frac{x_3}{\sqrt{y_3^2+x_3^2}}\right),$$

$$\theta_1(t)=\arccos\left(\frac{x_2\beta^2+\sqrt{(1+\beta^2)r^2(t)-x_2^2\beta^2}}{(1+\beta^2)r(t)}\right),$$

$$\theta_2(t)=\arccos\left(\frac{x_2\beta^2-\sqrt{(1+\beta^2)r^2(t)-x_2^2\beta^2}}{(1+\beta^2)r(t)}\right),$$

$$\theta_3(t)=\arccos\left(\frac{x_3}{r(t)}\right).$$

V. FIELDS FROM TRIANGLES AND SQUARES

In conclusion a few examples of use of these equations are shown. The first example is for a triangle and shows the spatial impulse response for point locations as indicated in the top graph in Fig. 8. A mesh plot is shown in Fig. 8, and the responses indicated by a cross and a circle is shown in Fig. 9. The height above the plane is $z=60$ mm and the speed of sound is 1540 m/s. It is seen how the reaching of an edge by the spherical wave is accompanied by a discontinuity in the response at the corresponding time. Note that the number of discontinuities varies with the field position, and that there are at most five discontinuities.

The field in the second example in Fig. 10 stems from a rectangle divided into four triangles. This example is shown for reference and is compared to the equations for a rectangle. The height above the plane is 60 mm and the speed of sound is 1540 m/s. The same response is obtained for both calculations.

The triangular shape is ideally suited as the basic shape for modeling complex three-dimensional shapes, as is done in nearly all finite element programs. The derivation of the response from a triangle, thus, makes it possible to create a general acoustic field program as the one described in Ref. 1 using triangles instead of squares.

[1] J. A. Jensen and N. B. Svendsen, ''Calculation of pressure fields from arbitrarily shaped, apodized, and excited ultrasound transducers,'' IEEE Trans. Ultrason. Ferroelectr. Frequency Control **39**, 262–267 (1992).

[2] G. R. Harris, ''Review of transient field theory for a baffled planar piston,'' J. Acoust. Soc. Am. **70**, 10–20 (1981).

[3] G. E. Tupholme, ''Generation of acoustic pulses by baffled plane pistons,'' Mathematika **16**, 209–224 (1969).

[4] P. R. Stepanishen, ''Transient radiation from pistons in an infinite planar baffle,'' J. Acoust. Soc. Am. **49**, 1629–1638 (1971).

[5] P. R. Stepanishen, ''The time-dependent force and radiation impedance on a piston in a rigid infinite planar baffle,'' J. Acoust. Soc. Am. **49**, 841–849 (1971).

[6] A. Penttinen and M. Luukkala, ''The impulse response and nearfield of a curved ultrasonic radiator,'' J. Phys. D **9**, 1547–1557 (1976).

[7] M. Arditi, F. S. Forster, and J. Hunt, ''Transient fields of concave annular arrays,'' Ultrason. Imag. **3**, 37–61 (1981).

[8] J. C. Lockwood and J. G. Willette, ''High-speed method for computing the exact solution for the pressure variations in the nearfield of a baffled piston,'' J. Acoust. Soc. Am. **53**, 735–741 (1973).

[9] A. D. Pierce, *Acoustics, An Introduction to Physical Principles and Applications* (Acoustical Society of America, New York, 1989), pp. 213–217.

Downloaded¬28¬Jun¬2010¬to¬192.38.67.112.¬Redistribution¬subject¬to¬ASA¬license¬or¬copyright;¬see¬http://asadl.org/journals/doc/ASALIB-home/info/ter

[10] P. M. Morse and K. U. Ingard, *Theoretical Acoustics* (McGraw-Hill, New York, 1968).
[11] L. E. Kinsler, A. R. Frey, A. B. Coppens, and J. V. Sanders, *Fundamentals of Acoustics* (Wiley, New York, 1982), 3rd ed., pp. 165–169.
[12] P. R. Stepanishen, ''Pulsed transmit/receive response of ultrasonic piezoelectric transducers,'' J. Acoust. Soc. Am. **69**, 1815–1827 (1981).
[13] J. A. Jensen, ''A model for the propagation and scattering of ultrasound in tissue,'' J. Acoust. Soc. Am. **89**, 182–191 (1991).

Downloaded¬28¬Jun¬2010¬to¬192.38.67.112.¬Redistribution¬subject¬to¬ASA¬license¬or¬copyright;¬see¬http://asadl.org/journals/doc/ASALIB-home/info/ter